Thermal conductivity and sound velocities of hydrogen-silsesquioxane low-k dielectrics

Ruxandra M. Costescu, Andrew J. Bullen, George Matamis,* Keith E. O'Hara,† and David G. Cahill‡
Department of Materials Science and Engineering, Coordinated Science Laboratory, and Materials Research Laboratory, University of Illinois, Urbana, Illinois 61801
(Received 17 August 2001; published 15 February 2002)

Thermal conductivities of hydrogen-silsesquioxane thin films—Dow Corning ''flowable oxide'' and nanoporous ''extra-low-k'' spin-on dielectrics—are measured in the temperature range 80–400 K using the 3ω method. Film thickness and atomic densities are characterized by the combination of Rutherford-backscattering spectrometry and variable-angle spectroscopic ellipsometry. Measurements of the longitudinal speeds of sound by picosecond ultrasonics and interferometry enable comparisons with the model of the minimum thermal conductivity of homogeneous materials. This model fails to capture the strong temperature dependence of the conductivity. Data for nanoporous silsesquioxane and SiO_2 are compared to the predictions of effective medium theories of heterogeneous materials. Differential-effective-medium theory predicts a scaling of thermal conductivity Λ with atomic density n, $\Lambda \propto n^{3/2}$ in good agreement with experiment. The comparisons with effective-medium theories suggest that a greater control of pore microstructure may enable significant improvements in the thermal and mechanical properties of porous dielectrics.

DOI: 10.1103/PhysRevB.65.094205 PACS number(s): 66.70.+f, 44.30.+v, 61.43.−j, 68.60.−p

I. INTRODUCTION

At temperatures $T > 100$ K, the thermal conductivities[1] of most amorphous dielectrics with homogeneous microstructures are well described by the minimum thermal conductivity, a model originally proposed by Einstein[2] and extended by others [1,3,4] to include heat transport by a broader spectrum of vibrational modes. More rigorous theories[5,6] successfully predict the thermal conductivity of disordered materials when the atomic bonding and microstructure are well understood; a calculation of the minimum thermal conductivity Λ_{min}, however, requires knowledge of only the atomic density and speeds of sound.[1] Recently, we tested the applicability of Λ_{min} for understanding the thermal conductivity of a wide variety of amorphous carbon[7] thin films and found good agreement between the data and the predictions of the model. Atomic bonding and hydrogen content—and therefore, the atomic density and sound velocity—vary dramatically with deposition method and these changes in microstructure cause the thermal conductivity Λ of a-C:H to span a wide range, $0.2 < \Lambda < 2.5$ W m^{-1} K^{-1}.

By contrast, if the microstructure of a material is manipulated by introducing porosity rather than by changes in the local atomic structure, we cannot expect that a Debye model based on the average atomic density n and macroscopic sound velocity v will adequately describe the spectrum of heat-carrying vibrational modes; therefore, the model of the minimum thermal conductivity may fail to adequately capture the magnitude and temperature dependence of the thermal conductivity. Instead, we must consider effective-medium theories[8–10] for heterogeneous materials to gain insight on the thermal and mechanical properties. Fortunately, the extremely short coherence lengths of the dominant heat-carrying vibrational modes[5,6] makes the application of effective-medium theories to the conductivity of amorphous materials appropriate even when the length scale of the porosity is only a few nanometers.

To explore these effects of porosity on the thermal conductivity of amorphous materials, we have investigated the thermal conductivity of hydrogen-silsesquioxane (HSQ) films in the temperature range $80 < T < 400$ K. HSQ films are under intense investigation by the microelectronics industry as so-called ''spin-on low-k dielectrics;'' dielectrics with relative dielectric constant $k < 4.0$ decrease propagation delay, signal cross talk, and power dissipation relative to the traditional dielectric SiO_2.[11,12] (Power dissipation is reduced during switching because the use of low-k dielectrics increases the ac impedance of the interconnects.) Low k is, therefore, a highly desirable property for intermetal dielectrics but, in general, low-k dielectrics also have reduced thermal conductivity and elastic constants, raising potential problems for thermal management and processing.

The effects of porosity on the room-temperature thermal conductivity of xerogel, a nanoporous form of a-SiO_2, were recently studied by Hu and co-workers.[13] They proposed phenomenological two-phase mixture models that usefully describe the dependence of the conductivity on porosity. We review the xerogel data[13] below together with our data for HSQ and previous studies of silica aerogels[14] and porous Vycor. [15,16]

II. EXPERIMENTAL DETAILS

Two forms of HSQ films on Si substrates were supplied by Dow-Corning: ''Flowable oxide'' (FOx), and ''extra low-k'' (XLK). The nominal composition of HSQ is $HSiO_{1.5}$. FOx is a relatively dense form of HSQ ($\rho \approx 1.4$ g cm^{-3}) with $k \approx 2.9$. FOx films are prepared by spin-coating HSQ resin in a carrier solvent, followed by melting and flowing, and, finally, by curing the film at 300–450 °C in N_2 ambient. The theoretical density[17] of fully dense HSQ is thought to be comparable to the density of a-SiO_2, $\rho = 2.2$ g cm^{-3}; the lower density of FOx films is not fully understood but may arise from the open volume at the center of cagelike molecular structures.[17,18]

XLK is a nanoporous form of HSQ with density ρ

≈ 0.9 g cm^{-3} and dielectric constant $k \approx 2.0$. Pores are intentionally introduced in the HSQ matrix through a three-step process: gellation in the presence of a high-boiling-point solvent at ambient conditions; removal of the solvent without collapsing the resin structure; and formation of a strong network during curing.[19] Gellation occurs when the film is exposed to an ammonia-and-moisture environment for 30–120 s, which causes SiH bonds to react with the H_2O to form SiOH; SiOH bonds then combine to form a SiOSi gel.[19–21] The distribution of pore sizes[21,20] of XLK films is thought be be strongly peaked at $d \approx 3$ nm.

We measure the thermal conductivity of FOx and XLK thin films using the 3ω method.[22–24] A narrow, thin-film metal line is used simultaneously as the heater and thermometer in the experiment; an ac current at frequency ω heats the line and sample at frequency 2ω, and the resulting oscillations in temperature and resistance give a small voltage signal at 3ω. For a film that is thermally thin (the thermal penetration depth in the film is large compared to its thickness h) and whose thermal conductivity is small compared to that of the substrate, the thin film simply adds a frequency-independent temperature oscillation to the thermal response of the substrate. Since h is small compared to the width w of the metal line and the thermal penetration depth in the substrate is large compared to w, heat flow is essentially one-dimensional in the thin film and radial in the substrate. We apply a small correction[23,25] for finite film thickness by replacing the true width of the heater/thermometer line w by an effective width $w_{\text{eff}} = w + 0.88h$.

We deposit the heater/thermometer metal films by sputter deposition and define the pattern using photolithography. We use Al lines with $w \approx 10$ μm for FOx samples. XLK films are damaged by our standard chemical etching process for Al; therefore, for XLK, we use Cu lines with $w \approx 30$ μm. A 5 nm layer of SiO_2 deposited by rf sputtering is used to improve the adhesion between XLK and Cu. Samples were made from five different FOx films (FOx-*A*, -*B*, -*C* and FOx-14, -15), and from two XLK films (XLK-6, cured at 450 °C; and XLK-15, cured at 425 °C). New data for two additional thin-film materials are also included below for comparisons: (i) an a-SiO_2 thin film deposited on a ceramic AlN substrate by rf sputtering of a silica target; and (ii) a sample of methyl-siloxane spin-on glass supplied by Allied-Signal (now Honeywell), Accuglass formulation 314.

Film thickness h and index of refraction are extracted from optical modeling of spectroscopic variable-angle ellipsometry data. Rutherford-backscattering spectrometry (RBS) gives the atomic areal densities σ and we combine ellipsometry and RBS results to calculate the average atomic density of Si and O atoms, $n = (\sigma_{\text{Si}} + \sigma_{\text{O}})/h$.

We obtain the longitudinal speeds of sound in FOx and XLK thin films from picosecond ultrasonics[26] and picosecond interferometry,[27–29] respectively. In picosecond ultrasonics, an opaque metal film, typically Al, deposited on the sample surface, partially absorbs a sub-picosecond optical pump pulse and generates an acoustic pulse that propagates away from the surface. The acoustic pulse reflects from interfaces in the sample and returns to the surface of metal film where the arrival time is detected by changes in the reflected intensity of a time-delayed optical probe pulse. In our experiments, the pump and probe pulses are generated by a mode-locked Ti:sapphire laser operating at $\lambda \approx 790$ nm. The speed of sound is calculated by the time τ that separates acoustic echoes from the Al/FOx and FOx/Si interfaces and the thickness h of the FOx film, $v_l = 2h/\tau$.

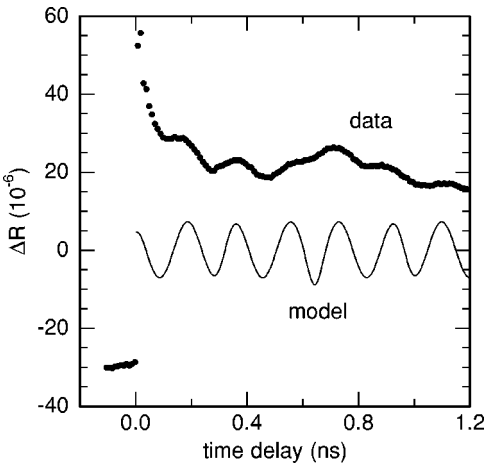

FIG. 1. Time-resolved changes in the reflectivity ΔR of sample XLK-6 at wavelength $\lambda \approx 790$ nm as a function of the time after excitation by a 0.5-ps pump pulse. The surface of the sample is coated with ≈ 10 nm of Pd. The large jump in ΔR at $t = 0$ is caused by the heating of the Pd film by the pump pulse. The modulation in the reflectivity with a period of ~ 0.2 ns is modeled by interference from a broadened acoustic pulse traveling in the XLK sample, see Eqs. (1) and (2). The acoustic pulse reflects from the XLK/Si interface at $t = 0.32$ ns and the surface at $t = 0.64$ ns.

Unfortunately, picosecond ultrasonics gave poorly defined echoes from the XLK/Si interface because of the large acoustic reflectivity of the Al/XLK interface and possibly because of significant acoustic attenuation in the XLK layer. We, therefore, applied picosecond interferometry to determine v_l. In picosecond interferometry,[27,28] the propagation of an acoustic pulse in a transparent sample is observed by the interference pattern of light scattered from the acoustic pulse, see Fig. 1. In our geometry,[29] we coat the sample film with a thin, ≈ 10 nm, semitransparent Pd film that absorbs the pump pulse and launches an acoustic wave into the sample.

Because the thickness of our XLK samples is comparable to one-half of the optical wavelength, the interferometry data include multiple reflections of the acoustic pulse from the substrate and surface and, as a consequence, analysis of the reflectivity data is not straightforward. We write the optical reflectivity of the sample R in terms of the Fresnel reflection coefficient [29] of the static sample r_0 and the Fresnel reflection coefficient of the acoustic pulse r_{sound}

$$R = R_0 + \Delta R = |r_0 + r_{\text{sound}}|^2 \approx |r_0|^2 + 2\,\text{Re}[r_0 r_{\text{sound}}]. \quad (1)$$

The time evolution of r_{sound} is calculated using[28,29]

$$r_{\text{sound}} = \frac{A}{\lambda} \int \eta(z) \exp\left(\frac{i 4\pi n z}{\lambda}\right) dz, \quad (2)$$

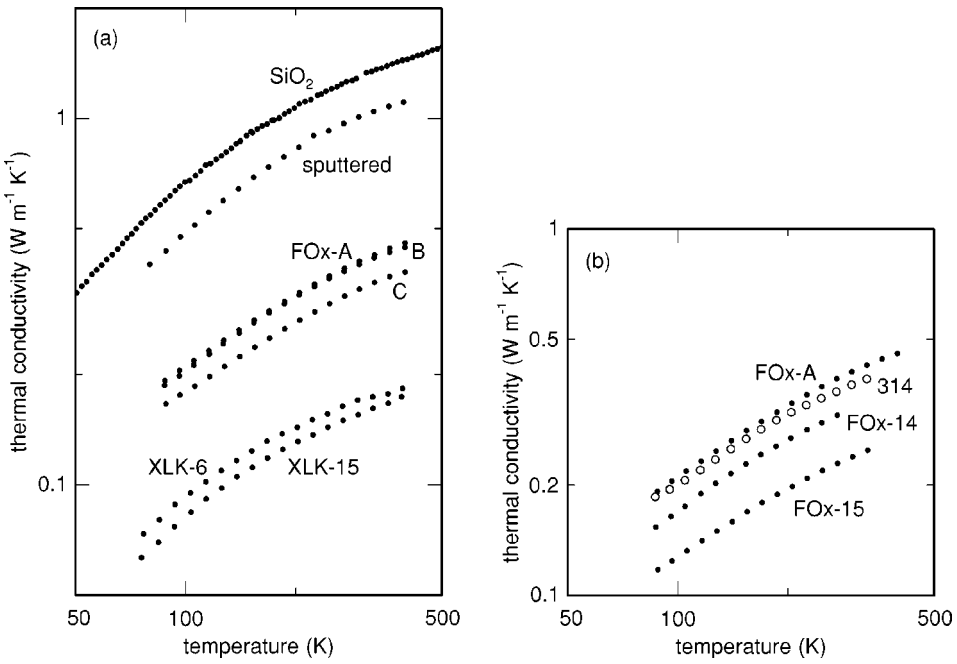

FIG. 2. (a) Thermal conductivity of FOx and XLK HSQ thin films. Data for bulk SiO_2, Ref. 22, and a thin film of SiO_2 deposited by rf sputtering are included for comparison. The three FOx samples were supplied by Dow-Corning in 1998 and are labeled by the letters *A*, *B*, and *C*; data for samples FOX-*A* and FOX-*B* nearly overlap. (b) Thermal conductivity of two FOx samples (FOx-14 and FOx-15) supplied in 1997. Data for a methyl-siloxane spin-on glass (open circles, Accuglass formulation 314) and sample FOx-*A* are included for comparison.

where n is the index of refraction, z the distance normal to the film surface, λ the laser wavelength, $\eta(z)$ the strain in the acoustic pulse[29] that propagates with velocity v_l, and A a complex coefficient that we adjust to fit the data. [The periodicity of ΔR is only weakly dependent on the shape of the strain pulse $\eta(z)$ but the positions of maxima and minima depend on the shape and the relative phases of the complex coefficients r_0 and r_{sound}. We, therefore, treat the complex constant A as an adjustable parameter.]

We assume that the acoustic reflection coefficient of the XLK/Si interface is ≈ 1 and that the acoustic pulse reflects from the sample surface with a change of sign. The interferometry signal is then antisymmetric about the time of the acoustic reflection from the XLK/Si interface and symmetric about the time of the acoustic reflection from surface. An example of this model calculation is included with the data in Fig. 1. This simple model does not include the acoustic or optical effects of the thin Pd layer,[29] acoustic attenuation,[28] or the displacement of interfaces during the reflections of the acoustic pulse.[29,30]

III. RESULTS AND DISCUSSION

Figure 2 shows the results of our thermal conductivity measurements on eight samples of spin-on dielectrics. (Data for samples FOx-14 and FOx-15 were reported previously[31] in a conference proceedings and are reproduced here for completeness.) The temperature dependence of the data is nearly identical for all samples; i.e., the conductivity of HSQ is suppressed relative to SiO_2 by a constant factor, which is independent of the temperature in the temperature range of our experiments, $80 < T < 400$ K. While the FOx samples show substantial variability, the data for four out of the five samples are within $\pm 10\%$ of 0.37 W m^{-1} K^{-1} at 300 K, a factor of ≈ 3.5 smaller than SiO_2. Data for XLK are a factor of ≈ 8 smaller than SiO_2. Table I lists the physical properties for room temperature. The data are consistent with previous reports of the thermal conductivity of HSQ,[11] the biaxial modulus of FOx,[18] the Young's modulus of XLK,[19] and c_{11} for methyl-siloxane.[32]

With increasing porosity, we find an increasingly poor match between the data and the model of the minimum thermal conductivity, see Fig. 3. The minimum thermal conductivity[1] $\Lambda_{\min}$ is derived from Einstein's theory of heat transport[2] and the Debye model of lattice vibrations by dividing the material into regions of size $\lambda/2$ that oscillate with frequency $\omega = 2\pi v/\lambda$. The lifetime of the oscillators is $\tau = \pi/\omega$

$$\Lambda_{\min} = \left(\frac{\pi}{6}\right)^{1/3} k_B n^{2/3} \sum_{i=1}^{3} v_i \left(\frac{T}{\Theta_i}\right)^2 \int_0^{\Theta_i/T} \frac{x^3 e^x}{(e^x-1)^2}\, dx. \quad (3)$$

The sum is taken over the two transverse and one longitudinal sound modes of velocity v_i with a cutoff frequency for each polarization (expressed in K) of $\Theta_i = v_i(\hbar/k_B)(6\pi^2 n)^{1/3}$.

Because porosity decreases the average atomic density n and sound velocity v—and therefore also decreases the cutoff frequency Θ_i—the Debye model underlying Eq. (3) greatly underestimates the true upper bound of the spectrum of lattice vibrations of a porous solid; e.g., for XLK, $\Theta_t \approx 80$ K and $\Theta_l \approx 135$ K are a factor of ≈ 6 smaller than the corresponding cutoff frequencies for SiO_2. Furthermore, since the temperature dependence of $\Lambda_{\min}$ derives from the quantum-mechanical heat capacity of the vibrational modes, when $\Theta_i < 150$ K, $\Lambda_{\min}$ has negligible temperature dependence for $T > 80$ K, see Fig. 3.

The nearly identical temperature dependence of the thermal conductivities of SiO_2, FOx, and XLK suggests that the spectrum of heat-carrying vibrational modes is nearly the same in all three materials. (We have previously shown that this is also true for porous Vycor.[15]) We can then explore the

TABLE I. Numerical values for the physical properties of the samples in this study. Film thickness and optical index of refraction at a wavelength of 790 nm are measured by spectroscopic, variable-angle ellipsometry. With knowledge of the film thickness, we measure the longitudinal sound velocity v_l by picosecond ultrasonics and picosecond interferometry; the atomic density of Si atoms n_{Si} by Rutherford-backscattering spectrometry; and the thermal conductivity Λ by the 3ω method. Thermal conductivity data are listed for near room temperature 298 K.

Sample	Thickness (nm)	Optical index at 790 nm	v_l (nm ps^{-1})	n_{Si} (10^{22} cm^{-3})	Λ (W m^{-1} K^{-1})
Bulk SiO_2		1.454	5.97	2.20	1.35
Sputtered SiO_2	212	1.49	5.65	2.00	1.00
FOx-*A*	285	1.41	2.35	1.69	0.40
FOx-*B*	470	1.42	2.30	1.70	0.40
FOx-*C*	775	1.39	1.85	1.54	0.33
FOx-14	215	1.41	2.65	1.79	0.34
FOx-15	375	1.41	2.00	1.68	0.24
XLK-6	498	1.22	1.55	1.02	0.170
XLK-15	508	1.26	1.65	1.04	0.155
SOG-314	270	1.46	3.20	2.01	0.38

applicability of effective medium theories for heterogeneous materials, treating the porous solid as a composite material of a matrix punctuated by voids. Landauer[9] has provided an excellent review of the long and interesting history of effective-medium theories; following Ref. 9, in Fig. 4 we compare our conductivity data to three theoretical approaches, all of which were known more than 60 years ago. These theories are rigorous in the limit of small concentrations and also in the limit of large concentrations when the contrast between matrix and second phase is small.[10] Our system, a two-phase composite of voids of zero-thermal con-

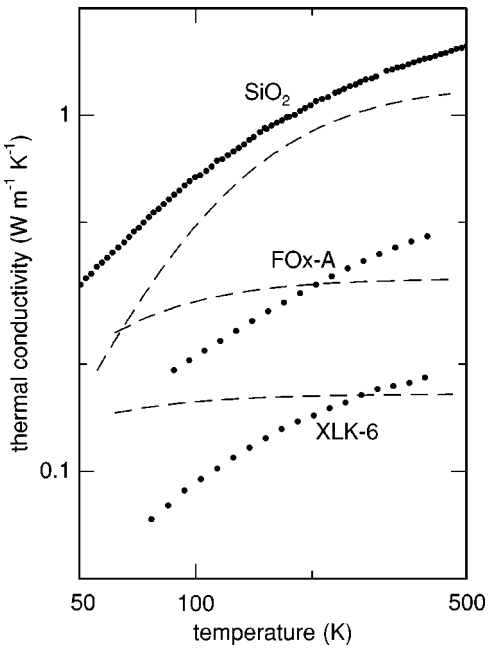

FIG. 3. Comparison of data for HSQ and SiO_2 (filled circles) to calculations of the minimum thermal conductivity using Eq. (3) (dashed lines) for each material. Since the transverse speed of sound v_t for the HSQ samples is unknown, we set $v_t = 0.60 v_l$.

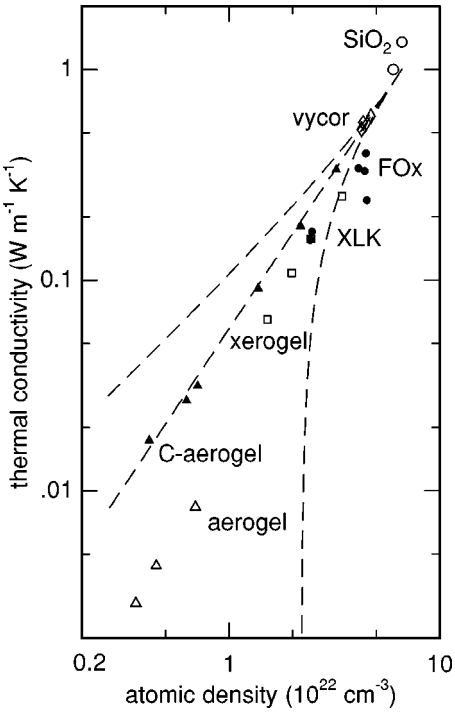

FIG. 4. Summary of the room-temperature thermal conductivity of hydrogen-silsesquioxane films (solid circles labeled by FOx and XLK) and various forms of SiO_2 plotted as a function of the atomic density of Si and O atoms. Data for the lattice conductivity of carbon aerogels (filled triangles, Ref. 33) are included for comparison. Data for SiO_2 are from the literature: SiO_2 (open circles, Ref. 22); porous Vycor (diamonds, Refs. 15 and 16); xerogel (open squares, Ref. 13); and the lattice conductivity of silica aerogel (open triangles, Ref. 14). The three dashed lines are effective-medium theories for a composite of a matrix material with $\Lambda_m = 1$ W m^{-1} K^{-1} and voids. From upper left to lower right, these theories are the Clausius-Mossotti approximation, the differential effective medium theory, and the coherent potential approximation, see Eqs. (4)–(6).

ductivity in a thermally conductive matrix, cannot be treated exactly; we examine these theories with the intent of learning which, if any, provides a useful, approximate description of the thermal conductivity of porous dielectrics.

The Clausius-Mossotti (CM) approximation is also the basis of the Maxwell-Garnett theory of optical constants[9] and equivalent to the upper bound for an isotropic composite derived by Hashin.[8] The conductivity of a periodic cellular solid[34]—i.e., a porous solid with an ordered arrangement of identical pores—is also known to be comparable to this upper bound. For a matrix of thermal conductivity Λ_m and density n_m, the Clausius-Mossotti equation for the effective thermal conductivity Λ of the porous material of average density n reduces to

$$\frac{\Lambda_{\mathrm{CM}}}{\Lambda_m}=\frac{2\left(\frac{n}{n_m}\right)}{3-\left(\frac{n}{n_m}\right)}. \tag{4}$$

The differential-effective-medium (DEM) theory is also known as the asymmetric or unsymmetric Bruggeman[9,35] theory. By introducing an infinitesimal volume fraction of spherical voids, applying the CM approximation to find the change in conductivity and integrating the result

$$\frac{\Lambda_{\mathrm{DEM}}}{\Lambda_m}=\left(\frac{n}{n_m}\right)^{3/2}. \tag{5}$$

The coherent potential (CP) approximation is also known as the symmetric Bruggeman theory,[35] an approach derived independently by Landauer.[36] This equation is symmetric in the two components and predicts a percolation threshold at a density $(n/n_m)=1/3$

$$\frac{\Lambda_{\mathrm{CP}}}{\Lambda_m}=\frac{1}{2}\left[3\left(\frac{n}{n_m}\right)-1\right]. \tag{6}$$

Clearly, the DEM theory, Eq. (5), provides the best description of the dependence of the data on density, see Fig. 4. We have set the conductivity of the matrix $\Lambda_m=1$ W m^{-1}K^{-1} to fit data for porous Vycor because n_m for Vycor is well known, but almost perfect agreement with data for low-k films could easily be achieved by adjusting the conductivity of the matrix Λ_m to fit the data for FOx, XLK, and xerogel; then, $\Lambda_m=0.70$ W m^{-1}K^{-1}. DEM theory has also proven valuable in other situations when the contrast in the properties of the two phases is large; e.g., the acoustic properties of sedimentary rock[37] and the microwave conductivity of metal/dielectric mixtures.[38]

While our primary concern is the thermal conductivity of porous dielectrics, we also consider the usefulness of effective-medium theories for understanding the elastic constants. Sound velocity data are summarized in Fig. 5. Effective-medium theories for the elastic constants are significantly more complex than theories for conductivity or susceptibility but some simplification[10,39] results when $K_m=4G_m/3$, where K_m is the bulk modulus of the matrix and G_m the shear modulus. We have chosen $G_m=24$ GPa and

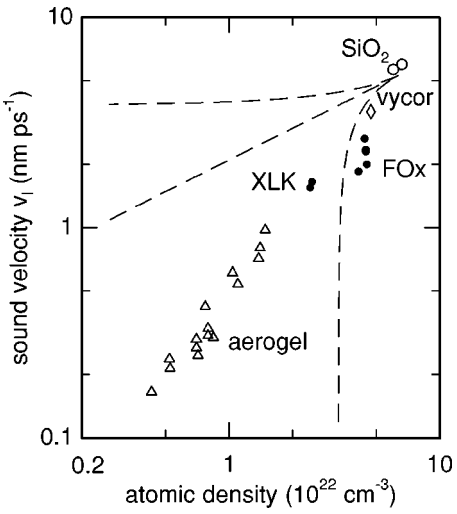

FIG. 5. Summary of the longitudinal sound velocity of hydrogen-silsesquioxane films (solid circles labeled by FOx and XLK) and various forms of SiO_2 plotted as a function of the atomic density of Si and O atoms. Data for SiO_2 are from the literature: SiO_2 (open circles, Ref. 28); porous Vycor (diamonds, Ref. 41), and silica aerogel (open triangles, Ref. 40). The three dashed lines are effective-medium theories for a composite of a matrix material (bulk modulus $K=32$ GPa, shear modulus $G=24$ GPa) and voids. From upper left to lower right, these theories are the upper bound derived in Ref. 42; the differential-effective-medium theory, Ref. 10; and the coherent potential approximation, Ref. 39.

$K_m=32$ GPa to model the matrix properties, see Fig. 5. (For pure a-SiO_2, $G=31$ GPa and $K=37$ GPa.) In this case, the coupled-effective-medium equations[8,10,39] for G and K separate and are similar to the equations for conductivity

$$\frac{G_{\mathrm{CM}}}{G_m}=\frac{\frac{n}{n_m}}{2-\left(\frac{n}{n_m}\right)}, \tag{7}$$

$$\frac{G_{\mathrm{DEM}}}{G_m}=\left(\frac{n}{n_m}\right)^2, \tag{8}$$

$$\frac{G_{\mathrm{CP}}}{G_m}=2\left(\frac{n}{n_m}\right)-1. \tag{9}$$

We calculate the longitudinal sound velocity from $\rho v_l^2=8G/3$ where ρ is the mass density, and compare the results to the data plotted in Fig. 5. None of these approaches adequately describes the sound velocity data. The experimental values appear to scale as a power law $v_l \propto n^{1.4}$ (as previously noted by Fricke and co-workers [40]) but the exponent is much larger than predicted by the DEM theory, $v_l \propto n^{1/2}$, see Eq. (8).

IV. CONCLUSIONS

For applications of low-k HSQ films in microelectronics, the thermal conductivity Λ and the elastic constants should

be as large as possible to minimize problems of thermal management and processing by chemical mechanical polishing. We have shown that Λ is in reasonably good agreement with DEM theory,[9,35] see Eq. (5) and Fig. 4. But the comparisons of Fig. 4 also demonstrate that some modest improvement in Λ may be possible with changes in the pore microstructure: for values of the density n near that of XLK, the upper bound to the conductivity given by Eq. (4) is $\approx$40% greater than the DEM theory. This improvement might be achieved by pore microstructures with greater order; the conductivity of a periodic cellular solid[34] is comparable to the upper bound. Given that the sound velocities are far below even the predictions of the DEM theory, see Fig. 5, we speculate that ordering of the pore microstructure could produce even more dramatic improvements in the mechanical properties.

ACKNOWLEDGMENTS

We thank H.-C. Liou and W. Chen (Dow Corning) for supplying FOx and XLK samples, A. Bharde (Honeywell) for samples of methyl-siloxane spin-on glass, and C. Hu (Intel) for sharing thermal conductivity data for xerogel. We also thank K. Samiee for his improvements of the data acquisition software for the pump-probe experiments and T. Schwarz-Selinger for selected translations of Ref. 35. This work was supported by NSF Grant No. CTS 99-78822. Sample characterization by RBS, ellipsometry, and picosecond ultrasonics used the facilities of the Center for Microanalysis of Materials, supported by U.S. DOE Grant No. DEFG02-91ER45439.

*Present address: San Disk Corp., 9600 Godwin Dr., Manassas, VA 20110.

†Present address: Integrated Micromachines Inc., 1400 S. Shamrock Ave., Monrovia, CA 91016.

‡Electronic address: d-cahill@uiuc.edu

[1] D. G. Cahill, S. K. Watson, and R. O. Pohl, Phys. Rev. B **46**, 6131 (1992).

[2] A. Einstein, Ann. Phys. (Leipzig) **35**, 679 (1911).

[3] C. Kittel, Phys. Rev. **75**, 972 (1948).

[4] G. A. Slack, in *Solid State Physics*, edited by F. Seitz and A. G. Turnbull (Academic Press, New York, 1979), Vol. 34, pp. 1 and 57.

[5] P. B. Allen and J. L. Feldman, Phys. Rev. B **48**, 12 581 (1993).

[6] J. L. Feldman, M. D. Kluge, P. B. Allen, and F. Wooten, Phys. Rev. B **48**, 12 589 (1993).

[7] A. J. Bullen, K. E. O'Hara, and D. G. Cahill, J. Appl. Phys. **88**, 6317 (2000).

[8] Z. Hashin, J. Compos. Mater. **2**, 284 (1968).

[9] R. Landauer, in *Electrical Transport and Optical Properties of Inhomogeneous Media*, edited by J. C. Garland and D. B. Tanner (AIP, New York, 1978), pp. 2–43.

[10] J. G. Berryman, J. Acoust. Soc. Am. **91**, 551 (1992).

[11] W. W. Lee and P. S. Ho, MRS Bull. **22**, 19 (1997).

[12] J. L. Hedrick, R. D. Miller, C. J. Hawker, K. R. Carter, W. Volksen, D. Y. Yoon, and M. Trollsas, Adv. Mater. **10**, 1049 (1998).

[13] C. Hu, M. Morgen, P. S. Ho, A. Jain, W. N. Gill, J. L. Plawsky, and P. C. Wayner, Appl. Phys. Lett. **77**, 145 (2000).

[14] J. Fricke, X. Lu, P. Wang, D. Büttner, and U. Heinemann, Int. J. Heat Mass Transf. **35**, 2305 (1992).

[15] D. G. Cahill, R. H. Tait, R. B. Stephens, S. K. Watson, and R. O. Pohl, in *Thermal Conductivity*, edited by C. J. Cremers and H. A. Fine (Plenum, New York, 1990), Vol. 21, pp. 3–16.

[16] S. K. Watson, Ph.D. thesis, Cornell University, 1992.

[17] M. P. Petkov, M. H. Weber, K. G. Lynn, K. P. Rodbell, and S. A. Cohen, J. Appl. Phys. **86**, 3104 (1999).

[18] J.-H. Zhao, I. Malik, T. Ryan, E. T. Ogawa, P. S. Ho, W.-Y. Shih, A. J. McKerrow, and K. J. Taylor, Appl. Phys. Lett. **74**, 944 (1999).

[19] C. Jin and J. Wetzel, in Proceedings of the 2000 International Interconnect Technology Conference (IITC), Burlingame, CA, pp. 99–101.

[20] E. S. Moyer, K. Chung, M. Spaulding, T. Deis, R. Boisvert, C. Saha, and J. Bremmer, in Proceedings of the 2000 International Interconnect Technology Conference (IITC) (Ref. 19), pp. 196–197.

[21] R. A. Donaton *et al.*, in Proceedings of the 2000 International Interconnect Technology Conference (IITC) (Ref. 19), pp. 93–95.

[22] D. G. Cahill, Rev. Sci. Instrum. **61**, 802 (1990).

[23] D. G. Cahill, M. Katiyar, and J. R. Abelson, Phys. Rev. B **50**, 6077 (1994).

[24] S.-M. Lee and D. G. Cahill, J. Appl. Phys. **81**, 2590 (1997).

[25] T. Borca-Tasciuc, A. R. Kumar, and G. Chen, Rev. Sci. Instrum. **72**, 2139 (2001).

[26] C. Thomsen, H. T. Grahn, H. J. Maris, and J. Tauc, Phys. Rev. B **34**, 4129 (1986).

[27] C. Thomsen, H. T. Grahn, H. J. Maris, and J. Tauc, Opt. Commun. **60**, 55 (1986).

[28] H.-N. Lin, R. J. Stoner, H. J. Maris, and J. Tauc, J. Appl. Phys. **69**, 3816 (1991).

[29] K. E. O'Hara, X.-Y. Hu, and D. G. Cahill, J. Appl. Phys. **90**, 4852 (2001).

[30] O. B. Wright, J. Appl. Phys. **71**, 1617 (1992).

[31] S.-M. Lee, G. Matamis, D. G. Cahill, and W. P. Allen, Microscale Thermophys. Eng. **2**, 31 (1998).

[32] G. Carlotti, G. Socino, and L. Doucet, Appl. Phys. Lett. **66**, 2682 (1995).

[33] X. Lu, O. Nilsson, J. Fricke, and R. W. Pekala, J. Appl. Phys. **73**, 581 (1993).

[34] A. G. Leach, J. Phys. D **26**, 733 (1993).

[35] D. A. G. Bruggeman, Ann. Phys. (Leipzig) **24**, 636 (1935).

[36] R. Landauer, J. Appl. Phys. **23**, 779 (1952).

[37] P. Sheng, Phys. Rev. B **41**, 4507 (1990).

[38] W. M. Merrill, R. E. Diaz, M. M. LoRe, M. C. Squires, and N. G. Alexopoulos, IEEE Trans. Antennas Propag. **47**, 142 (1999).

[39] B. Budiansky, J. Mech. Phys. Solids **13**, 223 (1965).

[40] J. Gross, J. Fricke, R. W. Pekala, and L. W. Hrubesh, Phys. Rev. B **45**, 12 774 (1992).

[41] J. J. De Yoreo, Ph.D. thesis, Cornell University, 1985.

[42] Z. Hashin, J. Appl. Mech. **29**, 143 (1962).